Dienophile Cycloaddition to Cycloheptatriene and Related Complexes of Tricarbonyliron. *X*-Ray Crystal Structures of $[Fe(CO)_3(\eta^4\text{-}C_7H_7CN)]\cdot C_2(CN)_4$ and $[Fe(CO)_3(\eta^4\text{-}C_7H_7\text{–}C_7H_7)]$†

Suman K. Chopra, Desmond Cunningham, Seamus Kavanagh, Patrick McArdle,* and Grainne Moran
Chemistry Department, University College Galway, Galway, Ireland

The rate of tetracyanoethene (tcne) addition to tricarbonyliron complexes of some substituted azepines and 1-cyanocycloheptatriene have been measured. Experimental support for a concerted mechanism for the cycloaddition of tcne to tricarbonyl(η^4-cycloheptatriene)iron is provided by the high dienophile dependence of the observed reaction rate on changing from tcne to tricyanoethene. Frontier orbital theory successfully predicts that 1,3-addition is the reaction mode favoured for cycloaddition of tcne to a range of cyclic triene complexes of tricarbonyliron.

The cycloaddition of dienophiles to cyclic triene and tetraene complexes has been studied by several workers.[1–3] The assumption of a concerted nature for the addition of, for example, tetracyanoethene (tcne) to $[Fe(CO)_3(\eta^4\text{-chpt})]$ (**1a**) (chpt = cycloheptatriene), to give the '1,3-adduct' (**2a**) has been justified on the basis of solvent effects on the rate of addition. The small solvent effects observed discounted a dipolar intermediate. The application of orbital symmetry rules to these and related reactions[1] suggested that it might also be possible to apply frontier orbital theory to these systems. Since a valid application of frontier orbital theory to cycloaddition reactions is only possible if the reaction has a concerted mechanism, it was decided to extend the kinetic studies and to re-examine the concertedness of the reaction.

Results and Discussion

Addition of Tetracyanoethene to Substituted (η^4-Azepine)-tricarbonyliron Complexes.—Tricarbonyl(η^4-*N*-ethoxycarbonylazepine)iron, (**1b**), has been reported to react with tcne to give a 1,3-adduct which then isomerised to a 1,6-adduct, Scheme 1.[4] The rate of this addition has been measured in CH_2Cl_2 and $MeNO_2$ solution and the results are given in Tables 1 and 2. There is only a two-fold increase in rate on going to the more polar solvent, a much greater increase would be expected if a dipolar intermediate were involved, and this modest increase is consistent with a concerted mechanism for the reaction.

It was not possible due to solubility problems to follow the reactions of (**1c**) or (**1d**) by ^1H n.m.r. spectroscopy. Mössbauer spectra can readily distinguish the σ,η^3 mode of bonding in (**2**) from the η^4 bonding in (**1**) and (**3**). The former show small quadrupole splittings <0.9 mm s^{-1} while the latter have quadrupole splittings >1.2 mm s^{-1}.[5] It was hoped that this technique would be able to indicate if initial 1,3-addition took place for (**1c**) and (**1d**). Solutions of (**1b**) and (**1c**) with 10:1 mol ratios of tcne to metal complex were frozen in liquid nitrogen 3 min after mixing. Solutions of tcne and (**1d**) in acetone with the same mol ratio were frozen after 3 h at 25 °C. Spectra of these frozen solutions are compared with results obtained for isolated solid samples in Table 3.

(η^4-3-Acetylazepine)tricarbonyliron (**1c**) reacts with tcne to give a 1:1 adduct (**3c**). The rate of this addition is given in Tables 1 and 2; there is an intercept on the second-order plot. The Mössbauer results indicate that a 1,3-adduct is an intermediate in this reaction. The reaction was followed by i.r. using the ν(MC–O) bands. Solutions with 1:1, 3:1, and 10:1 molar ratios of tcne to (**1c**) were examined. It was only in the latter case that all of the absorptions due to (**1c**) were

Table 1. Observed rate constants for addition of tcne at 25 °C

Complex	10^3[tcne]/mol dm^{-3}	$10^2k_{obs.}$/s^{-1}	Solvent
(**1b**)[a,b]	2.12	2.2	CH_2Cl_2
	3.87	4.3	
	6.17	6.7	
	7.80	8.7	
	10.04	11.8	
(**1b**)[a,c]	2.11	6.0	$MeNO_2$
	4.13	11.6	
	6.19	17.30	
	8.10	22.40	
	8.66	24.10	
(**1c**)[a,d]	1.95	30.2	CH_2Cl_2
	3.99	50.3	
	5.99	72.1	
	8.03	92.5	
	9.93	112.2	
(**1e**)[e]	16.0	3.29×10^{-2}	CH_2Cl_2
	24.0	3.73×10^{-2}	
	32.0	4.37×10^{-2}	
	40.0	4.85×10^{-2}	
	48.0	5.36×10^{-2}	

[a] Concentration 2.5×10^{-4} mol dm^{-3}. [b] Measured on stopped-flow apparatus at 395 nm. [c] Measured on stopped-flow apparatus at 415 nm. [d] Measured on stopped-flow apparatus at 420 nm. [e] Concentration 2×10^{-4} mol dm^{-3}; measured on PE 983G instrument at 2 056 cm^{-1}.

Table 2. Second-order rate constants for tcne additions at 25 °C

Complex	Slope (k_1/dm^3 mol^{-1} s^{-1})	Intercept (k_{-1}/s^{-1})	Solvent
(**1b**)	11.89 ± 0.36		CH_2Cl_2
(**1b**)	27.47 ± 0.12		$MeNO_2$
(**1c**)	$(10.32 \pm 0.82) \times 10^1$	$(9.79 \pm 0.54) \times 10^{-2}$	CH_2Cl_2
(**1e**)	$(6.57 \pm 0.23) \times 10^{-3}$	$(2.22 \pm 0.47) \times 10^{-4}$	CH_2Cl_2

† Tricarbonyl(1—4-η-1-cyanocycloheptatriene)iron–tetracyanoethene (1/1) and [1—4-η-bi(cycloheptatrienyl)]tricarbonyliron respectively.

Supplementary data available: see Instructions for Authors, *J. Chem. Soc., Dalton Trans.*, 1987, Issue 1, pp. xvii—xx.

Non-S.I. unit employed: eV ≈ 1.60×10^{-19} J.

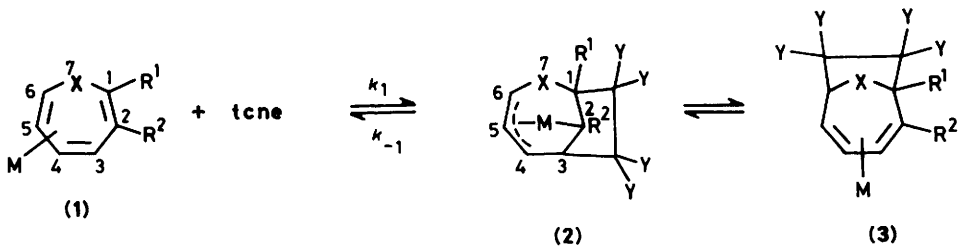

(1) (2) (3)

Scheme 1. M = $Fe(CO)_3$, Y = CN; (**a**) X = CH_2, R^1 = R^2 = H; (**b**) X = NCO_2Et, R^1 = R^2 = H; (**c**) X = NH, R^1 = H, R^2 = COMe; (**d**) X = NCO_2Et, R^1 = H, R^2 = COMe; (**e**) X = CH_2, R^1 = CN, R^2 = H; (**f**) X = CO, R^1 = R^2 = H; (**g**) M = $Fe(CO)_2(PPh_3)$, X = CH_2, R^1 = R^2 = H

Table 3. Iron-57 Mössbauer spectra (mm s^{-1})[a]

Complex	δ[b]	Δ[c]
(**3b**)[d]	0.28	1.33
(**2b**) + (**3b**)[e]	0.27 + 0.28	0.86 + 1.33
(**3c**)[d]	0.31	1.38
(**2c**) + (**3c**)[e]	0.31 + 0.30	1.38 + 0.72
(**2d**) + (**3d**)[d]	0.29 + 0.27	0.70 + 1.35
(**2d**) + (**3d**)[e]	0.29 + 0.27	0.70 + 1.35

[a] Source at 25 °C, sample at −196 °C; values are ±0.05 mm s^{-1}. [b] Chemical shift relative to sodium nitroprusside, $Na_2[Fe(CN)_5(NO)]$. [c] Quadrupole splitting. [d] Isolated crystalline solid. [e] Frozen acetone solution.

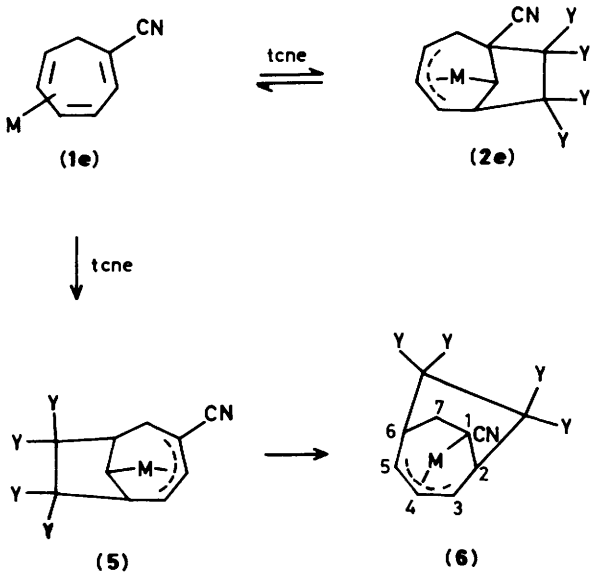

(1e) (2e) (5) (6)

Scheme 2. M = $Fe(CO)_3$, Y = CN

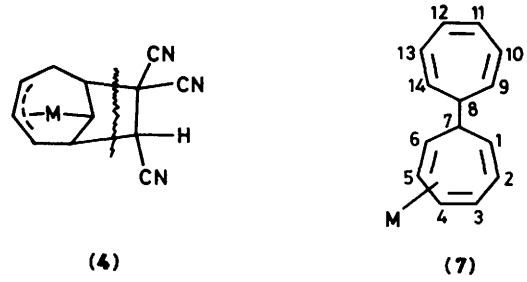

(4) (7)

M = $Fe(CO)_3$

removed on addition of tcne. There is clearly an equilibrium between (**1c**) and tcne and the initial adduct formed in solution. If excess of 4-isopropyl-1-methylcyclohexa-1,3-diene (imchxd), which reacts rapidly and irreversibly with tcne,[4] is added to separate reacting solutions of (**1c**) and tcne after 3 min and after 10 min then 70% and 15% of the original (**1c**) is regenerated respectively. These results are interpreted in terms of Scheme 1. Complex (**1c**) and tcne react in a reversible manner to form (**2c**) which irreversibly isomerizes at a slower rate, k_2, to the 1,6-adduct (**3c**). The ν(MC–O) bands of (**2c**) and (**3c**) were coincident. The slope of the second-order plot is k_1 and the intercept is k_{-1}. The rate law for this scheme is $k_{obs.} = k_2K[tcne]/(1 + K[tcne])$. The alternative possibility that (**3c**) is formed by direct interaction of (**1c**) and tcne, $k_{2'}$, and not by isomerization of (**2c**), cannot be ruled out as the rate law for this would be $k_{obs.} = k_{2'}[tcne]/(1 + K[tcne])$ and in both cases a plot of $1/k_{obs.}$ *vs.* 1/[tcne] gives a straight line with an intercept. While kinetic results cannot distinguish these two possibilities the latter is considered unlikely on the basis of the n.m.r. results reported for (**1b**)[4] and the frontier orbital predictions below. The electron-withdrawing acetyl group adjacent to C^1 is probably responsible for labilizing the 1,3-adduct. A similar effect has been reported for tricarbonyl(η^4-1-formylcycloheptatriene)iron.[2]

(η^4-3-Acetyl-*N*-ethoxycarbonylazepine)tricarbonyliron, (**1d**), reacts with tcne to give a 1:1 adduct. The rate of this addition however was too slow, at reasonable tcne concentrations, for accurate kinetic work ($k_{obs.} = 2.33 \times 10^{-3}$ s^{-1}, [tcne] = 3.5×10^{-2} mol dm^{-3}). Infrared spectra clearly show that the addition is irreversible in this case. The Mössbauer results suggest that 1,3- and 1,6-adducts are in equilibrium in this case and that both crystallize from solution.

Addition of Tetracyanoethene to Tricarbonyl(η^4-1-*cyanocycloheptatriene*)*iron*, (**1e**).—This complex reacted with tcne in dichloromethane solution to give a 1:1 adduct. When equimolar quantities of (**1e**) and tcne were allowed to react in CH_2Cl_2 solution for 2 d the i.r. spectrum indicated that the reaction had not gone to completion. When this solution was treated with excess of imchxd (**1e**) slowly reformed. The rate of this reaction was followed by i.r. spectroscopy. The results are given in Tables 1 and 2. The slope of the second-order plot is assigned to the rate of 1,3-addition and the intercept to the reverse of this reaction, (**2e**) to (**1e**). When the reaction was monitored by n.m.r. over a longer period (two weeks at 25 °C) absorptions due to two new complexes, (**5**) and (**6**), were observed. The crystal structure of (**6**) is described below. Scheme 2 suggests a reasonable explanation for the formation of (**6**) by isomerization of (**5**). It is clearly the presence of the electron-withdrawing cyanide group that makes tcne additon to (**1e**) the slowest addition rate measured for any tricarbonyliron com-

plex. Despite this deactivation initial electrophilic attack still takes place at the unco-ordinated side of the molecule. The n.m.r. spectrum of (**1e**) in trifluoroacetic acid clearly showed that protonation also takes place at the unco-ordinated side of the molecule, *i.e.* the C^1 position.

The Mechanism of Cycloaddition.—It has been established by Huisgen and Schug[6] that a characteristic of the Diels–Alder type cycloaddition is the observation of a high dienophile dependence on the rate of addition. In contrast, cycloadditions involving an ionic intermediate show only a small rate change. Huisgen has used the (2 + 2) cycloaddition of dienophiles to enol ethers as examples of the latter type of reaction.[6]

To examine the dienophile dependence of reactions involving tricarbonyliron complexes, the rate of addition of tricyanoethene (trcne) to complexes (**1a**), (**1b**), and (**1g**) has been studied. In each case 1:1 adducts were isolated and satisfactory analytical data obtained. It was not possible to obtain n.m.r. spectra of these adducts due to solubility problems. The positions of the ν(MC–O) i.r. bands support the assignment of structure (**4**) to these adducts. First-order rate constants for these additions are given in Table 4 and the second-order rate constants are given in Table 5. Data from Huisgen's work are also included in Table 5 for comparison. Large reaction rate decreases are observed on going from tetra- to tri-cyanoethene for complexes (**1a**), (**1b**), and (**1g**). These data would therefore support the classification of these reactions with the Diels–Alder type and suggest a concerted mechanism for them.

Theoretical Calculations.—Extended Hückel calculations have been reported by Albright and co-workers[7] for (**1a**). The calculations were based on a planar geometry for the cycloheptatriene ligand. Since an accurate knowledge of the frontier orbital coefficients was required it was decided to carry out charge iterative calculations using the best available structural data. While good quality structural data are available for tropone (cycloheptatrienone) and azepine complexes the only reported structure for a cycloheptatriene complex is that of tricarbonyl(η^4-7-phenylcycloheptatriene)iron which was determined photographically and reported without hydrogen atom positions.[8] To provide more accurate data the structure of (**7**) was determined and is described below. Extended Hückel calculations were also carried out for tropone and some substituted azepine complexes. Details of the calculations are given in the Experimental section.

Atomic charges. Charge distributions, calculated using a model geometry derived from that of complex (**7**), Table 6, show that C^1, C^3, and C^6 are the most negative sites in co-ordinated cycloheptatriene and tropone ligands. However, even when C^1 carries an electron-withdrawing substituent (1-CN or 1-CHO),

Table 4. Observed rate constants for addition of trcne at 25 °C

Complex	10^2[trcne]/ mol dm^{-3}	$10^3 k_{obs.}$/s^{-1}	Solvent
(**1a**)[a,b]	1.94	1.78	CH_2Cl_2
	1.55	1.43	
	1.36	1.24	
	1.16	1.08	
	0.78	0.73	
	0.58	0.54	
	0.39	0.36	
(**1b**)[b]	0.80	1.10×10^{-1}	CH_2Cl_2
	1.20	1.65×10^{-1}	
	1.60	2.18×10^{-1}	
	2.00	2.70×10^{-1}	
	2.40	3.28×10^{-1}	
(**1g**)[c]	0.25	1.88×10^{-3}	CH_2Cl_2
	0.37	2.96×10^{-3}	
	0.50	3.81×10^{-3}	
	0.63	4.90×10^{-3}	
	0.75	5.70×10^{-3}	

[a] Concentration 2.5×10^{-3} mol dm^{-3}; measured on a Cary 17 instrument at 370 nm. [b] Concentration 1×10^{-3} mol dm^{-3}; measured on stopped-flow apparatus at 450 nm. [c] Concentration 3×10^{-4} mol dm^{-3}; measured on stopped-flow apparatus at 340 nm.

Table 6. Calculated carbon atomic charges

Complex	C^1	C^2	C^3	C^4	C^5	C^6	Method
(**1a**)	−0.027	−0.024	−0.20	0.005	0.003	−0.016	*a*
(**1b**)	0.004	0.001	−0.016	0.033	−0.003	0.032	*b*
(**1c**)	0.039	−0.005	−0.044	0.002	0.007	0.021	*b*
(**1e**)	0.005	0.003	−0.015	0.009	0.003	−0.003	*a*
(**1f**)	−0.006	0.003	−0.005	0.021	0.020	−0.003	*a*

[a] All-atom charge iteration. [b] Single-cycle calculation.

Table 7. Calculated h.o.m.o. coefficients

Complex	C^1	C^2	C^3	C^4	C^5	C^6	Model
(**1a**)	0.490	0.337	−0.389	−0.144	0.121	−0.171	(**7**)
(**1a**)	0.454	0.278	−0.575	−0.252	0.106	−0.098	Ref. 8
(**1b**)	0.301	0.429	−0.211	−0.194	0.195	0.108	*a*
(**1c**)	0.238	0.439	−0.204	−0.227	0.239	0.146	*b*
(**1e**)	0.403	0.239	−0.501	−0.231	0.098	−0.111	(**7**)
(**1f**)	0.361	0.297	−0.410	−0.230	0.197	0.142	*c*
(**1g**)	0.314	0.498	−0.186	−0.210	0.222	0.100	(**7**)

[a] S. M. Johnson and I. C. Paul, *J. Chem. Soc. B*, 1970, 1783. [b] M. G. Waite and G. A. Sim, *J. Chem. Soc. A*, 1970, 1009. [c] R. P. Hodge, *J. Am. Chem. Soc.*, 1964, **86**, 5429.

Table 5. Comparison of dienophile addition rates at 25 °C

Compound	Dienophile	10^5(Rate)/dm^3 mol^{-1} s^{-1}	Rate ratio tcne : trcne
Cyclopentadiene	tcne	4.3×10^2	90
	trcne	4.8	1
9,10-Dimethylanthracene	tcne	1.3×10^5	2 203
	trcne	5.9×10^1	1
Isobutenyl methyl ether	tcne	3.97×10^{-5}	1.66
	trcne	2.39×10^{-5}	1
(**1a**)	tcne	$(6.22 \pm 0.08) \times 10^{-4}$	682
	trcne	$(9.12 \times 0.08) \times 10^{-7}$	1
(**1b**)	tcne	$(1.19 \pm 0.04) \times 10^{-4}$	880
	trcne	$(1.35 \pm 0.01) \times 10^{-7}$	1
(**1g**)	tcne	$>12 \times 10^{-1}$	>156
	trcne	$(7.66 \pm 0.22) \times 10^{-3}$	1

Figure 1. H.o.m.o.–l.u.m.o. interactions

and C^6 then bears the most negative charge, initial 1,3-addition (and not 1,6-attack) is still the observed reaction. This suggests that the reaction is not charge controlled.

Frontier Orbital Interactions.—The important frontier orbital interaction is that between the lowest unoccupied molecular orbital (l.u.m.o.) of the dienophile and the highest occupied molecular orbital (h.o.m.o.) of the complex. The h.o.m.o. coefficients are listed in Table 7 and illustrated in Figure 1. The small coefficients calculated for C^4, C^5, and C^6 and the change in phase between C^5 and C^6 contrast with the results reported for the planar cycloheptatriene model. In the planar model all of the h.o.m.o. coefficients are of similar magnitude.[7] The symmetry calculated for the h.o.m.o. of (**1a**) is not critically dependent on the exact geometry chosen for the complex. In fact results obtained using the geometry of tricarbonyl(7-phenylcycloheptatriene)iron (with hydrogen atoms in calculated positions), Table 7, are closely related to those obtained using the geometry of the bi(cycloheptatrienyl) complex. The h.o.m.o. coefficients of the azepine and tropone complexes also show a reduction in size at C^4, C^5, and C^6 but retain the relative phases reported for the planar model, with that for C^6 positive. This effect is not due to geometry changes but appears to be caused by the introduction of a group at the 7-position which is conjugated to the ring π-system. Indeed replacing the NH group in the azepine structure by a CH_2 group restores the coefficient pattern calculated for (**1a**). It is clear from the h.o.m.o. coefficients in Table 7 that both 1,3- and 1,4-cycloadditions are symmetry allowed, *i.e.* have symmetry corresponding to the l.u.m.o. of tcne, Figure 1. The larger value calculated for the C^3 coefficient would predict that 1,3 is the favoured addition mode. Goldschmidt *et al.*[3] have observed 1,3- and 1,4-addition of tcne to (**1f**) in the ratio of 96:4. No evidence has been found for 1,4-addition of tcne to any other η^4-triene complex.

Direct 1,6-addition is predicted to be symmetry forbidden for tropone and azepine complexes. Even in (**1a**) where 1,6-addition is not forbidden the coefficient at C^6 is relatively small, so that this mode of reaction would still be unfavourable. Thus in agreement with experimental observations initial 1,3-attack takes place in all of the systems, for which mechanistic studies have been reported, and no evidence for direct 1,6-attack has ever been found.

It is notable that in the 1,3-addition of the unsymmetrically substituted dienophiles $(CF_3)_2C{=}C(CN)_2$ and $(CF_3)_2C{=}O$ to tricarbonyl(η^4-triene)iron complexes, only one isomer is observed with the CF_3-substituted carbon adding to C^1.[1] However, the coefficient difference between C^1 and C^3 is not large, and is very sensitive to geometry; therefore a reliable prediction of the preferred orientation of an unsymmetrical dienophile cannot be made.

It is clear that frontier orbital theory has considerable predictive power in this area. However, it is also the case that a reasonable geometry must be adopted for the complex.

Crystal Structure of Tricarbonyl(η^4-1-cyanocycloheptatriene)iron–Tetracyanoethene (1/1), (**6**).—Crystallographic data are given in Table 8 and details of data collection in the Experimental section. The structure was solved by direct methods and refined using SHELX.[9] The iron atom was refined anisotropically. Atomic co-ordinates, bond lengths and angles are given in Tables 9—11. The ORTEP drawing, Figure 2, clearly shows that the tcne group is bonded across positions 2 and 6 of the cycloheptatriene ring. The iron is bonded to the ring system *via* an η^3-allyl interaction to C(3), C(4), and C(5) and a σ-bond to C(1). The overall structure is comparable to that reported for the tcne adduct of (**1a**), compound (**2a**).[10] The carbonyl groups show only small deviations from linearity and the Fe–C distances are close to those reported for (**2a**). The cyano groups show no large deviations from linearity, the largest being 3°. In the structure reported for (**2a**) two of the cyano groups exhibit angles less than 173° and N • • • H contacts

Table 8. Crystal data

Complex	(**6**)	(**7**)
Crystal dimensions	0.35 × 0.45 × 0.2	0.35 × 0.3 × 0.3
Crystal system	Monoclinic	Triclinic
Space group	$P2_1/c$	$P\bar{1}$
a/Å	8.229(3)	6.676(2)
b/Å	12.852(4)	9.863(2)
c/Å	16.314(5)	11.696(3)
α/°	90.0	98.82(2)
β/°	111.14(1)	92.96(2)
γ/°	90.0	99.96(2)
Z	4	2
U/Å^3	1 609.21	747.12
$F(000)$	775.96	331.98
μ/cm^{-1}	25.19	26.94
λ(Mo-K_α)/Å	0.710 69	0.710 69
Reflections observed [$I > 3\sigma(I)$]	1 305	1 669
Variable parameters	117	150
Max. shift/e.s.d.	<0.001	<0.004
Residual peaks (e Å^{-3}) in final difference map	max. 0.34 min. 0.37	0.27 0.22
Goodness of fit	0.95	1.24
R^a	6.89	4.95
R'^b	7.46	5.32
g^c	0.0008	0.0013

^{a} $R = \Sigma||F_o| - |F_c||/\Sigma F_o$. ^{b} $R' = \Sigma w^{\frac{1}{2}}||F_o| - |F_c||/\Sigma w^{\frac{1}{2}}|F_o|$. ^{c} $w = [\sigma^2(F_o) + gF_o^2]^{-1}$.

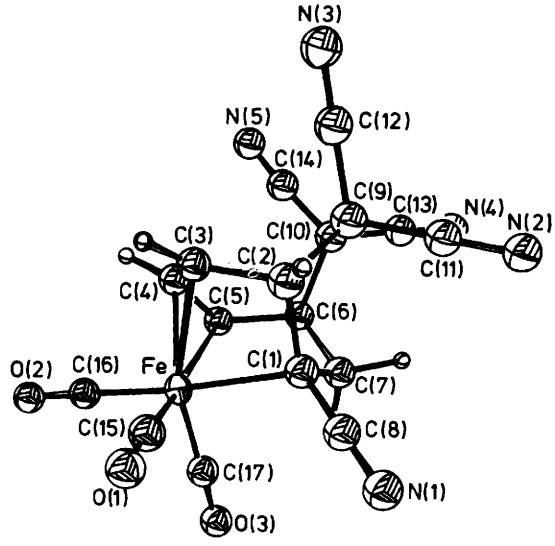

Figure 2. Crystal structure of (**6**)

Table 9. Fractional atomic co-ordinates for (**6**)

Atom	*x*	*y*	*z*	Atom	*x*	*y*	*z*
Fe	0.627 24(14)	0.220 17(10)	0.685 89(8)	C(5)	0.871 1(10)	0.302 3(6)	0.724 3(5)
O(1)	0.331 7(9)	0.097 5(6)	0.692 7(4)	C(6)	1.026 6(9)	0.227 3(6)	0.759 9(5)
O(2)	0.410 9(10)	0.399 5(6)	0.595 1(5)	C(7)	0.966 1(9)	0.114 7(6)	0.735 4(5)
O(3)	0.633 7(10)	0.139 5(6)	0.518 8(5)	C(8)	0.729 7(10)	0.001 8(7)	0.744 4(5)
N(1)	0.674 2(10)	−0.082 9(6)	0.733 9(5)	C(9)	1.011 0(10)	0.164 5(6)	0.909 3(5)
N(2)	1.027 2(10)	0.252 0(6)	1.056 4(5)	C(10)	1.117 2(11)	0.235 8(7)	0.863 4(5)
N(3)	1.137 7(9)	−0.022 1(6)	0.942 6(5)	C(11)	1.017 9(10)	0.214 0(6)	0.992 4(5)
N(4)	1.144 0(12)	0.424 6(7)	0.922 0(6)	C(12)	1.082 6(10)	0.059 9(6)	0.927 6(5)
N(5)	1.432 3(10)	0.160 2(7)	0.903 7(5)	C(13)	1.128 4(12)	0.341 1(7)	0.893 8(6)
C(1)	0.801 4(9)	0.105 4(6)	0.756 9(5)	C(14)	1.294 1(1)	0.194 2(7)	0.886 6(5)
C(2)	0.814 6(10)	0.153 7(6)	0.846 0(5)	C(15)	0.445 7(12)	0.147 4(8)	0.690 1(6)
C(3)	0.720 6(11)	0.257 9(7)	0.823 8(5)	C(16)	0.491 7(12)	0.329 2(7)	0.632 7(6)
C(4)	0.769 7(11)	0.330 5(7)	0.774 3(5)	C(17)	0.632 1(11)	0.172 0(7)	0.584 5(6)

Table 10. Bond lengths (Å) for (**6**)

Fe–C(1)	2.092(7)	Fe–C(3)	2.155(8)	C(1)–C(7)	1.522(10)	C(1)–C(8)	1.440(11)
Fe–C(4)	2.060(8)	Fe–C(5)	2.151(8)	C(2)–C(3)	1.523(12)	C(2)–C(9)	1.579(11)
Fe–C(15)	1.785(9)	Fe–C(16)	1.806(10)	C(3)–C(4)	1.387(12)	C(4)–C(5)	1.409(11)
Fe–C(17)	1.780(9)	O(1)–C(15)	1.149(11)	C(5)–C(6)	1.538(11)	C(6)–C(7)	1.536(12)
O(2)–C(16)	1.158(11)	O(3)–C(17)	1.154(10)	C(6)–C(10)	1.584(11)	C(9)–C(10)	1.623(11)
N(1)–C(8)	1.168(11)	N(2)–C(11)	1.130(10)	C(9)–C(11)	1.479(11)	C(9)–C(12)	1.455(11)
N(3)–C(12)	1.138(10)	N(4)–C(13)	1.156(12)	C(10)–C(13)	1.433(13)	C(10)–C(14)	1.467(12)
N(5)–C(14)	1.154(11)	C(1)–C(2)	1.548(10)				

Table 11. Bond angles (°) for (**6**)

C(3)–Fe–C(1)	70.4(3)	C(4)–Fe–C(1)	89.7(3)	C(4)–C(3)–C(2)	120.0(7)	C(3)–C(4)–Fe	74.5(5)
C(4)–Fe–C(3)	38.3(3)	C(5)–Fe–C(1)	78.7(3)	C(5)–C(4)–Fe	74.0(5)	C(5)–C(4)–C(3)	121.5(8)
C(5)–Fe–C(3)	69.0(3)	C(5)–Fe–C(4)	39.0(3)	C(4)–C(5)–Fe	67.0(5)	C(6)–C(5)–Fe	111.4(5)
C(15)–Fe–C(1)	91.4(4)	C(15)–Fe–C(3)	93.8(4)	C(6)–C(5)–C(4)	121.9(7)	C(7)–C(6)–C(5)	110.1(6)
C(15)–Fe–C(4)	127.4(4)	C(15)–Fe–C(5)	162.2(4)	C(10)–C(6)–C(5)	111.6(6)	C(10)–C(6)–C(7)	109.0(6)
C(16)–Fe–C(1)	173.9(4)	C(16)–Fe–C(3)	104.6(4)	C(6)–C(7)–C(1)	104.3(6)	C(1)–C(8)–N(1)	178.7(9)
C(16)–Fe–C(4)	84.2(4)	C(16)–Fe–C(5)	96.3(4)	C(10)–C(9)–C(2)	110.0(6)	C(11)–C(9)–C(2)	109.2(6)
C(16)–Fe–C(15)	92.6(4)	C(17)–Fe–C(1)	91.7(4)	C(11)–C(9)–C(10)	109.3(6)	C(12)–C(9)–C(2)	107.2(7)
C(17)–Fe–C(3)	158.4(4)	C(17)–Fe–C(4)	133.8(4)	C(12)–C(9)–C(10)	111.8(7)	C(12)–C(9)–C(11)	109.3(7)
C(17)–Fe–C(5)	96.3(4)	C(17)–Fe–C(15)	98.8(4)	C(9)–C(10)–C(6)	109.2(6)	C(13)–C(10)–C(6)	112.4(7)
C(17)–Fe–C(16)	92.3(4)	C(2)–C(1)–Fe	92.3(5)	C(13)–C(10)–C(9)	110.5(7)	C(14)–C(10)–C(6)	107.0(7)
C(7)–C(1)–Fe	107.8(5)	C(7)–C(1)–C(2)	114.7(6)	C(14)–C(10)–C(9)	108.9(7)	C(14)–C(10)–C(13)	108.7(7)
C(8)–C(1)–Fe	114.2(5)	C(8)–C(1)–C(2)	113.0(7)	C(9)–C(11)–N(2)	178.4(8)	C(9)–C(12)–N(3)	179.3(9)
C(8)–C(1)–C(7)	113.2(7)	C(3)–C(2)–C(1)	105.8(6)	C(10)–C(13)–N(4)	177.0(1)	C(10)–C(14)–N(5)	178.8(9)
C(9)–C(2)–C(1)	111.0(6)	C(9)–C(2)–C(3)	112.9(7)	O(1)–C(15)–Fe	177.7(9)	O(2)–C(16)–Fe	175.5(8)
C(2)–C(3)–Fe	90.5(5)	C(4)–C(3)–Fe	67.1(5)	O(3)–C(17)–Fe	179.0(8)		

of < 2.4 Å were observed. The shortest N ··· H contact found in the structure of (**6**) was H(3) ··· N(5) of 2.51 Å.

Crystal Structure of [η^4-*Bi(cycloheptatrienyl)*]*tricarbonyliron*, (**7**).—Crystallographic data are given in Table 8 and atomic co-ordinates, bond lengths and angles in Tables 12—14. The choice of the space group *P*1 was justified by the satisfactory subsequent refinement. The structure was solved by direct methods and refined using SHELX.[9] The iron atom and the three oxygen atoms were refined anisotropically. When all of the non-hydrogen atoms had been located, difference-Fourier maps clearly revealed the positions of the hydrogen atoms. Hydrogen atoms were included at these positions and were refined satisfactorily. The longest C–H bond was 1.17 Å and the shortest was 0.90 Å, Figure 3.

The structure is broadly similar to that reported for the 7-phenylcycloheptatriene complex.[8] The carbonyl groups show only small deviations from linearity (maximum 3°). The Fe–CO bond lengths are very similar, the largest deviation from the mean length being less than the experimental error. The co-ordinated ring is approximated by two planes folded about the C(3)–C(6) direction. The angle between the best planes defined by C(3),C(4),C(5),C(6) and C(6),C(7),C(1),C(2) is 44.2°. The iron atom is 1.59 Å below the former plane. The shortest bond in this ring is the C(1)–C(2) unco-ordinated double bond. The co-ordinated diene unit shows a slight bond alternation, C(4)–C(5) being just shorter than C(5)–C(6) and clearly shorter than C(3)–C(4). The unco-ordinated cycloheptatriene ring can be defined by three planes: C(9),C(10),C(13),C(14); C(8),C(9),C(14); C(10),C(11),C(12),C(13). The latter two are tilted out of the first by 53.3 and 25.7° respectively.

Experimental

Ultraviolet-visible spectra were recorded either on Cary 17 or Beckmann DB-GT spectrometers. Infrared spectra were obtained on a Perkin-Elmer 983G spectrometer. N.m.r. spectra were recorded on a JEOL MH-100 spectrometer. Kinetic measurements were made either on these spectrometers or on an Applied Photophysics stopped-flow device. All reaction rates were measured under pseudo-first-order conditions with excess dienophile. All reaction rates were checked for reproducibility and repeat runs with different solutions gave second-order rate

Table 12. Fractional atomic co-ordinates for (7)

Atom	*x*	*y*	*z*	Atom	*x*	*y*	*z*
Fe(1)	0.768 08(10)	0.229 20(6)	1.371 58(5)	C(8)	0.623 4(7)	0.319 0(5)	1.011 0(4)
O(1)	0.730 7(8)	0.520 6(4)	1.446 1(4)	C(9)	0.720 6(8)	0.207 5(5)	0.945 2(4)
O(2)	0.989 0(7)	0.166 7(5)	1.575 1(4)	C(10)	0.709 9(9)	0.184 3(6)	0.828 4(5)
O(3)	0.373 8(6)	0.089 0(5)	1.431 0(4)	C(11)	0.413 3(9)	0.755 6(6)	1.246 5(5)
C(1)	0.911 2(8)	0.426 2(5)	1.158 5(4)	C(12)	0.404 4(9)	0.280 7(6)	0.774 5(5)
C(2)	1.057 8(8)	9.396 9(5)	1.225 9(4)	C(13)	0.302 8(9)	0.264 4(6)	0.880 8(5)
C(3)	1.046 8(9)	0.283 0(6)	1.292 9(5)	C(14)	0.394 4(8)	0.273 2(5)	0.985 4(4)
C(4)	0.941 5(9)	0.141 3(6)	1.254 1(5)	C(15)	0.745 6(8)	0.406 5(6)	1.420 1(5)
C(5)	0.739 7(8)	0.116 0(6)	1.207 1(4)	C(16)	0.904 0(8)	0.188 9(5)	1.494 9(5)
C(6)	0.636 3(8)	0.228 6(5)	1.202 0(4)	C(17)	0.528 8(8)	0.142 6(5)	1.409 8(4)
C(7)	0.694 0(7)	0.353 9(5)	1.142 1(4)				

Table 13. Bond lengths (Å) for (7)

F(1)–C(3)	2.139(5)	Fe(1)–C(4)	2.032(6)	C(4)–H(4)	1.15(5)	C(5)–C(6)	1.412(8)
Fe(1)–C(5)	2.053(5)	Fe(1)–C(6)	2.127(5)	C(5)–H(5)	1.03(5)	C(6)–C(7)	1.514(7)
Fe(1)–C(15)	1.788(6)	Fe(1)–C(16)	1.797(6)	C(6)–H(6)	0.99(5)	C(7)–C(8)	1.549(6)
Fe(1)–C(17)	1.789(5)	O(1)–C(15)	1.143(7)	C(7)–H(7)	0.96(5)	C(8)–C(9)	1.504(7)
O(2)–C(16)	1.141(7)	O(3)–C(17)	1.136(7)	C(8)–C(14)	1.517(7)	C(8)–H(8)	1.12(5)
C(1)–C(2)	1.323(8)	C(1)–C(7)	1.490(7)	C(9)–C(10)	1.346(8)	C(9)–H(9)	1.07(5)
C(1)–H(1)	1.04(5)	C(2)–C(3)	1.459(7)	C(10)–H(10)	1.06(5)	C(12)–C(13)	1.463(8)
C(2)–H(2)	1.10(5)	C(3)–C(4)	1.445(8)	C(12)–H(12)	1.12(5)	C(13)–C(14)	1.323(8)
C(3)–H(3)	0.90(5)	C(4)–C(5)	1.394(8)	C(13)–H(13)	1.17(5)	C(14)–H(14)	0.97(5)

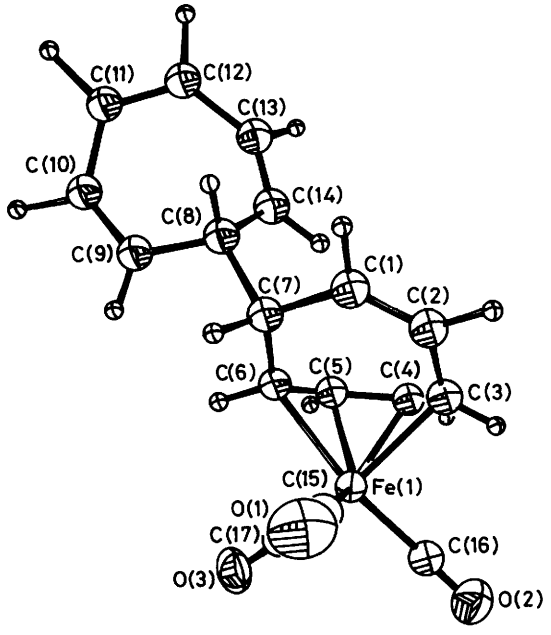

Figure 3. Crystal structure of (7)

constants within the experimental errors quoted. Rate constants were determined either from plots of $-\ln(A - A_\infty)$ against time or from Guggenheim plots. Temperature control was ±0.1 °C. The errors quoted were calculated as described by Swinbourne.[11] Complexes (**1a**), (**1b**), and (**1f**) and their tcne adducts were prepared by literature methods. Complexes (**1c**) and (**1d**) were prepared as described by Johnson and co-workers.[12] Tricyanoethene was prepared as described by Dickinson *et al.*[13] Dichloromethane was purified by repeated slow distillation; the final distillation under a nitrogen atmosphere was carried out immediately before use. Nitromethane was purified by distillation from P_2O_5 prior to use. All solutions were purged with nitrogen prior to their use.

Extended Hückel Calculations.—Calculations were carried out using the extended Hückel method;[14] the modified Wolfsberg-Helmholtz formula was used.[15] Charge-iterative calculations used the input parameters given in Table 15 for complexes with less than 25 atoms.[16] For the larger complexes, single-cycle calculations were used with H_{ii} values derived from the output of related charge-iterative calculations.

Crystal Structure Determination.—Crystallographic data were collected on a Hilger and Watts Y290 diffractometer. The software for operating the diffractometer was modified to suit random orientation work. The diffractometer was supervised by an Acorn BBC microcomputer, attached to both the serial line and the front panel of the PDP-8. An initial random orientation photograph was taken on a Weissenberg camera. The co-ordinates of the spots on this photograph were used by the system to compute θ and χ angles. The φ angle was found in the usual manner by rotation of φ. Refined angles were then used for cell reduction and Bravis lattice determination with BRVCEL.[17] Unit-cell dimensions were determined by a least-squares fit of θ values for 12 reflections which had $12 < \theta < 20°$. The angles used in the calculation were measured on the diffractometer. Data were corrected for Lorentz and polarization effects but not for absorption. The thermal parameters, U_{ij}, where in the form $\exp[-2\pi^2(U_{11}h^2a^{*2} + U_{22}k^2b^{*2} + U_{33}l^2c^{*2} + 2U_{12}hka^*c^* + 2U_{33}kb^*c^*)]$, and $U_{eq} = (U_{11} + U_{22} + U_{33})/3$.

The atomic scattering factors for non-hydrogen and hydrogen atoms and the anomalous dispersion correction factors for the non-hydrogen atoms were taken from the literature.[18–20] The equations for the planes described in the text were determined for both the mean and least-squares planes in all cases, with almost identical results. The maximum deviation for atoms defining the planes from the planes was 0.01 Å. All calculations were performed on either a DEC 2060, a VAX 11/785, or a BBC microcomputer. The ORTEP program was used to obtain the drawings.[21]

Tricarbonyl(η⁴-1-cyanocycloheptatriene)iron, (**1e**).—7-Cyanocycloheptatriene (0.3 mmol; prepared from tropylium

Table 14. Bond angles (°) for (7)

C(4)–F(1)–C(3)	40.4(2)	C(5)–Fe(1)–C(3)	71.7(2)	H(4)–C(4)–C(5)	122(2)	O(3)–C(17)–Fe(1)	177.7(5)
C(5)–Fe(1)–C(4)	39.9(2)	C(6)–Fe(1)–C(3)	82.7(2)	C(6)–C(5)–Fe(1)	73.1(3)	C(4)–C(5)–Fe(1)	69.2(3)
C(6)–Fe(1)–C(4)	71.5(2)	C(6)–Fe(1)–C(5)	39.5(2)	H(5)–C(5)–Fe(1)	120(3)	C(6)–C(5)–C(4)	119.9(5)
C(15)–Fe(3)–C(3)	94.2(2)	C(15)–Fe(1)–C(4)	132.2(2)	H(5)–C(5)–C(6)	122(3)	H(5)–C(5)–C(4)	117(3)
C(15)–Fe(1)–C(5)	130.5(2)	C(15)–Fe(1)–C(6)	92.9(2)	C(7)–C(6)–Fe(1)	120.1(3)	C(5)–C(6)–Fe(1)	67.4(3)
C(16)–Fe(1)–C(3)	91.1(2)	C(16)–Fe(1)–C(4)	94.5(2)	H(6)–C(6)–Fe(1)	113(3)	C(7)–C(6)–C(5)	128.4(4)
C(16)–Fe(1)–C(5)	124.8(2)	C(16)–Fe(1)–C(6)	164.3(2)	H(6)–C(6)–C(7)	111(3)	H(6)–C(6)–C(5)	111(3)
C(16)–Fe(1)–C(15)	124.8(2)	C(17)–Fe(1)–C(3)	164.7(2)	C(8)–C(7)–C(1)	109.8(4)	C(6)–C(7)–C(1)	117.4(4)
C(17)–Fe(1)–C(4)	102.0(2)	C(17)–Fe(1)–C(5)	94.2(2)	H(7)–C(7)–C(1)	110(3)	C(8)–C(7)–C(6)	111.4(4)
C(17)–Fe(1)–C(6)	90.2(2)	C(17)–Fe(1)–C(15)	99.6(3)	H(7)–C(7)–C(8)	98(3)	H(7)–C(7)–C(6)	108(3)
C(17)–Fe(1)–C(16)	92.3(2)	C(7)–C(1)–C(2)	126.4(5)	C(14)–C(8)–C(7)	114.0(4)	C(9)–C(8)–C(7)	113.7(4)
H(1)–C(1)–C(2)	119(3)	H(1)–C(1)–C(7)	114(3)	H(8)–C(8)–C(7)	104(2)	C(14)–C(8)–C(9)	106.8(4)
C(3)–C(2)–C(1)	128.1(5)	H(2)–C(2)–C(1)	120(3)	H(8)–C(8)–C(14)	107(3)	H(8)–C(8)–C(9)	111(3)
H(2)–C(2)–C(3)	112(3)	C(2)–C(3)–Fe(1)	116.4(4)	H(9)–C(9)–C(8)	119(3)	C(10)–C(9)–C(8)	121.4(5)
C(4)–C(3)–Fe(1)	65.8(3)	C(4)–C(3)–C(2)	125.6(5)	H(10)–C(10)–C(9)	110(3)	H(9)–C(9)–C(10)	120(3)
H(3)–C(3)–Fe(1)	107(3)	H(3)–C(3)–C(2)	118(3)	C(14)–C(13)–C(12)	126.0(5)	H(12)–C(12)–C(13)	126(3)
H(3)–C(3)–C(4)	111(3)	C(3)–C(4)–Fe(1)	73.8(3)	H(13)–C(13)–C(14)	114(3)	H(13)–C(13)–C(12)	118(3)
C(5)–C(4)–Fe(1)	70.9(3)	C(5)–C(4)–C(3)	119.8(5)	H(14)–C(14)–C(8)	123(3)	C(13)–C(14)–C(8)	122.4(5)
H(4)–C(4)–Fe(1)	121(2)	H(4)–C(4)–C(3)	117(2)	O(1)–C(15)–Fe(1)	177.0(5)	H(14)–C(14)–C(13)	114(3)
						O(2)–C(16)–Fe(1)	178.0(5)

Table 15. Input parameters for extended Hückel calculations

Atom	Orbital	H_{ii}/eV	z_1	z_2	C_1*	C_2*
Fe	3*d*	−13.0	5.35	1.80	0.5366	0.6678
	4*s*	−10.2	1.575			
	4*p*	−5.8	0.975			
C	2*s*	−21.4	1.625			
	2*p*	−11.4	1.625			
O	2*s*	−32.3	2.275			
	2*p*	−14.8	2.275			
N	2*s*	−26.0	1.95			
	2*p*	−13.4	1.95			
H	1*s*	−13.6	1.30			

* Contraction coefficients in the double-zeta expansion.

tetrafluoroborate and potassium cyanide), was reacted with $[Fe_2(CO)_9]$ (0.3 mmol) in toluene solution (50 cm^3) at reflux temperature for 1 h. This solution was allowed to cool and was placed on an alumina column. Toluene–ethyl acetate (3:1) eluted a yellow band which was evaporated *in vacuo* to give a yellow oil. This oil was treated with diethyl ether (30 cm^3) and 60% HPF_6 solution until no further precipitate formed. This salt was filtered and washed with diethyl ether. The salt in acetone solution was deprotonated with excess triethylamine. The neutral cyanide complex was extracted with diethyl ether–water, the organic layer separated, dried and evaporated to an oil. This oil was distilled onto a cold-finger where it crystallized to give (**1e**) in overall 20% yield (Found: C, 51.35; H, 2.75; N, 5.40. $C_{11}H_7FeNO_3$ requires C, 51.40; H, 2.35; N, 5.45%). The i.r. spectrum of (**1e**) contained ν(MC–O) bands at 2 056 and 1 989 cm^{-1} in CH_2Cl_2 solution. ^1H N.m.r. (CS_2 solution): δ 2.42 (dd, 2 H, H^7, $H^{7'}$, J = 1.5, 2.2), 3.00 (m, 1 H, H^6), 3.30 (m, 1 H, H^3), 5.38 (m, 2 H, H^4, H^5), and 6.62 p.p.m. (d, 1 H, H^2, J = 5.0 Hz)

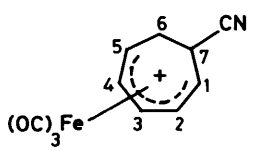

(Found: C, 32.55; H, 2.10; N, 3.40. $C_{11}H_8F_6FeNO_3P$ requires C, 32.75; H, 1.99; N, 3.50%). ^1H N.m.r. of (**1e**) in CF_3CO_2H–$CDCl_3$ solution: δ 1.08—1.5 (m, 3 H, H^6, $H^{6'}$, H^7), 3.16 + 3.32 [2 m, 2 H, H^1, H^5], 4.24 + 4.52 [2 m, 2 H, H^2, H^4], 5.40 p.p.m. [t, 1 H, H^3, J = 2 Hz]. The observation of only three protons at the higher field positions expected for protons on sp^3 carbons confirms that protonation has taken place at the 1-position of (**1e**).

[η⁴-*Bi(cycloheptatrienyl)*]*tricarbonyliron*, (**7**).—Tropylium tetrafluoroborate (2.0 g) was suspended in CH_2Cl_2 (50 cm^3). Complex (**1a**) (2.61 g) in CH_2Cl_2 (20 cm^3) was added. The mixture was stirred until all of the tropylium salt had dissolved. Diethyl ether (120 cm^3) was added dropwise with constant stirring and a yellow salt precipitated. This salt was stirred in acetone and treated with a saturated aqueous solution of sodium bicarbonate until the pH was >7. The mixture was extracted with diethyl ether–water. The organic layer was dried and evaporated *in vacuo* to an oil. This oil was allowed to dehydrate on a column of silica gel–toluene for 14 d. Toluene eluted a red band which was evaporated to an oil. This oil was essentially pure (**7**), overall yield 40% (Found: C, 63.75; H, 4.8. $C_{17}H_{14}FeO_3$ requires C, 63.35; H, 4.4%). Crystals were grown from toluene for crystallography. The i.r. spectrum (CH_2Cl_2) contained ν(MC–O) bands at 2 045 and 1 974 cm^{-1}.

Reactions with Tetracyanoethene.—Compound (**1c**) (0.25 g) and tcne (1.2 g) were stirred in dichloromethane solution under a nitrogen atmosphere for 3 min. Addition of hexane and removal of the solvent *in vacuo* gave crystals of (**2c**) mixed with some (**3c**). Longer reaction times gave pure (**3c**), yield 60%. Compounds (**2c**) and (**3c**) had identical ν(MC–O) i.r. bands at 2 021 and 2 076 cm^{-1} in CH_2Cl_2 solution. For (**3c**) (Found: C, 50.3; H, 2.4; N, 17.0. $C_{17}H_9FeN_5O_4$ requires C, 50.6; H, 2.2; N, 17.4%).

Compound (**1d**) (0.25 g) and tcne (0.9 g) were heated under reflux in dichloromethane solution for 90 min. When the i.r. spectrum indicated that all of the starting complex had reacted the solvent was removed *in vacuo*. Using an efficient sublimation apparatus (high vacuum and a liquid-nitrogen cooled cold-finger) excess tcne was removed at 40 °C. The residue was recrystallized from CH_2Cl_2–hexane to give a mixture of (**2d**) and (**3d**) which had identical ν(MC–O) i.r. bands at 2 023 and 2 084 cm^{-1} in CH_2Cl_2 solution. These complexes could not be separated. For (**2d**)/(**3d**) (Found: C, 50.2; H, 2.7; N, 14.3. $C_{20}H_{13}FeN_5O_6$ requires C, 50.5; H, 2.75; N, 14.8%).

Compound (**1e**) (0.5 g) and tcne (0.6 g) were allowed to react in CH_2Cl_2 solution for 24 h at 25 °C. Slow addition of hexane precipitated the adduct. Excess tcne was removed *in vacuo* to give the product in 80% yield. The i.r. spectrum of (**2e**) contained

ν(MC–O) bands at 2 083 and 2 023 cm^{-1} in CH_2Cl_2 solution (Found: C, 52.65; H, 2.30; N, 18.0. $C_{17}H_7FeN_5O_3$ requires C, 53.00; H, 1.80; N, 18.20%). ^1H N.m.r. ([$^2H_6$]acetone): δ 1.92 (d, 1 H, H^2, J = 4), 2.06 (m, 2 H, H^7, $H^{7'}$), 3.56 (m, 1 H, H^3), 4.76 (m, 1 H, H^6), 5.22 p.p.m. (m, 2 H, H^4, H^5). After 2 weeks in [$^2H_6$]acetone solution the n.m.r. spectrum was that expected for the 2,5-adduct, (**6**): δ 2.42 (2 m, 2 H, H^7, $H^{7'}$), 3.94 (m, 1 H, H^6), 4.42 (d, 1 H, H^2, J = 4.5), 4.84 (t, 1 H, H^3, J = 4.5 Hz), 5.50 p.p.m. (m, 2 H, H^4, H^5). There was no high field resonance typical of a proton attached to a carbon σ-bonded to a metal.

Reactions with Tricyanoethene.—Complex (**1a**) (0.1 g) and trcne (0.05 g) were stirred in CH_2Cl_2 under nitrogen at 25 °C. After 60 min, the solvent was removed *in vacuo* at room temperature. The product was recrystallized from hexane–CH_2Cl_2 to give the product in 50% yield (Found: C, 53.60; H, 2.60; N, 12.85. $C_{15}H_9FeN_3O_3$ requires C, 53.70; H, 2.70; N, 12.5%). The mass spectrum of this adduct contained a parent peak at *m/e* 355 and peaks for the loss of three CO groups. The i.r. spectrum in CH_2Cl_2 solution contained peaks at 2 080 and 2 018 cm^{-1}.

Complex (**1b**) was reacted with trcne in a similar manner to that described for (**1a**) to give a 1:1 adduct in 60% yield (Found: C, 49.95; H, 3.00; N, 13.75. $C_{17}H_{12}FeN_4O_5$ requires C, 50.00; H, 2.95; N, 13.75%). The i.r. spectrum of this adduct in CH_2Cl_2 solution contained peaks at 2 070 and 2 010 cm^{-1}.

Complex (**1g**) was reacted with trcne in a similar manner to that described for (**1a**) to give a 1:1 adduct in 50% yield (Found: C, 67.45; H, 4.40; N, 7.30. $C_{32}H_{24}FeN_3O_2P$ requires C, 67.50; H, 4.40; N, 7.40%). The i.r. spectrum of this adduct in CH_2Cl_2 solution contained peaks at 1 990 and 1 935 cm^{-1}.

References

1 M. Green, S. M. Heathcock, T. W. Turney, and D. M. P. Mingos, *J. Chem. Soc., Dalton Trans.*, 1977, 204.
2 S. K. Chopra, M. J. Hynes, and P. McArdle, *J. Chem. Soc., Dalton Trans.*, 1981, 586.
3 Z. Goldschmidt, H. E. Gottlieb, and D. Cohen, *J. Organomet. Chem.*, 1985, **294**, 219.
4 S. K. Chopra, G. Moran, and P. McArdle, *J. Organomet. Chem.*, 1981, **214**, C36.
5 D. Cunningham, P. McArdle, H. Sherlock, B.F.G. Johnson, and J. Lewis, *J. Chem. Soc., Dalton Trans.*, 1977, 2340.
6 R. Huisgen and R. Schug, *J. Am. Chem. Soc.*, 1976, **98**, 7819.
7 K. J. Karel, T. A. Albright, and M. Brookhart, *Organometallics*, 1982, **1**, 419.
8 J. A. D. Jeffreys and C. Metters, *J. Chem. Soc., Dalton Trans.*, 1977, 729.
9 G. M. Sheldrick, SHELX, computer program for crystal structure determination, University of Cambridge, 1976.
10 J. Weaver and P. Woodward, *J. Chem. Soc. A*, 1971, 3521.
11 E. S. Swinbourne, 'Analysis of Kinetic Data,' Nelson, London, 1971, p. 41.
12 G. B. Gill, N. Gourlay, A. W. Johnson, and M. Mahendran, *Chem. Commun.*, 1969, 631.
13 C. L. Dickinson, D. W. Wiley, and B. C. McKuisick, *J. Am. Chem. Soc.*, 1960, **82**, 6132.
14 J. Howell, A. Rossi, D. Wallace, K. Haraki, and R. Hoffman, FORTICON 8, Quantum Chemistry Program Exchange, University of Indiana, Bloomington, 1974, no. 344.
15 J. H. Ammeter, H. B. Burgi, J. G. Thibeault, and R. Hoffmann, *J. Am. Chem. Soc.*, 1978, **100**, 3686.
16 D. G. Carroll, A. T. Armstrong, and S. P. McGlynn, *J. Chem. Phys.*, 1966, **44**, 1865.
17 T. Higgins, M. Mahon, P. McArdle, and J. Simmie, BRVCEL, program for cell reduction and Bravis lattice determination, University College Galway, Ireland, 1985.
18 D. T. Cromer and J. B. Mann, *Acta Crystallogr., Sect. A*, 1968, **24**, 321.
19 R. F. Stewart, E. R. Davidson, and W. T. Simpson, *J. Chem. Phys.*, 1965, **42**, 3175.
20 D. T. Cromer and D. J. Liberman, *J. Chem. Phys.*, 1970, **53**, 1891.
21 C. K. Johnson, ORTEP, report ORNL 3794, Oak Ridge National Laboratory, Tennessee, 1965, revised 1971.

Received 23*rd December* 1986; *Paper* 6/2471